

# Ciclopirox ethanolamine preserves the immature state of human HSCs by mediating intracellular iron content

Mehrnaz Safaee Talkhoncheh,<sup>1</sup> Aurélie Baudet,<sup>1,\*</sup> Fredrik Ek,<sup>2,\*</sup> Agatheeswaran Subramaniam,<sup>1</sup> Yun-Ruei Kao,<sup>3</sup> Natsumi Miharada,<sup>1</sup> Christine Karlsson,<sup>1</sup> Leal Oburoglu,<sup>1</sup> Anna Rydström,<sup>1</sup> Kristijonas Zemaitis,<sup>1</sup> Abdul Ghani Alattar,<sup>1</sup> Justyna Rak,<sup>1</sup> Kristian Pietras,<sup>4</sup> Roger Olsson,<sup>2</sup> Britta Will,<sup>3,5</sup> and Jonas Larsson<sup>1</sup>

<sup>1</sup>Molecular Medicine and Gene Therapy, Lund Stem Cell Center, and <sup>2</sup>Chemical Biology and Therapeutics, Department of Experimental Medical Science, Lund University, Lund, Sweden; <sup>3</sup>Department of Cell Biology, Albert Einstein College of Medicine, Bronx, NY; <sup>4</sup>Division of Translational Cancer Research, Medicon Village, Lund University, Lund, Sweden; and <sup>5</sup>Department of Medicine (Oncology), Albert Einstein College of Medicine, Bronx, NY

## Key Points

- CPX is a regulator of HSCs and preserves the stem cell state in culture.
- CPX-induced HSC maintenance is mediated by intracellular iron chelation, which restricts respiratory capacity and proliferation.

Culture conditions in which hematopoietic stem cells (HSCs) can be expanded for clinical benefit are highly sought after. To elucidate regulatory mechanisms governing the maintenance and propagation of human HSCs *ex vivo*, we screened libraries of annotated small molecules in human cord blood cells using an optimized assay for detection of functional HSCs during culture. We found that the antifungal agent ciclopirox ethanolamine (CPX) selectively supported immature CD34<sup>+</sup>CD90<sup>+</sup> cells during culture and enhanced their long-term *in vivo* repopulation capacity. Purified HSCs treated with CPX showed a reduced cell division rate and an enrichment of HSC-specific gene expression patterns. Mechanistically, we found that the HSC stimulating effect of CPX was directly mediated by chelation of the intracellular iron pool, which in turn affected iron-dependent proteins and enzymes mediating cellular metabolism and respiration. Our findings unveil a significant impact of iron homeostasis in regulation of human HSCs, with important implications for both basic HSC biology and clinical hematology.

## Introduction

Development of strategies to preserve and expand functional human hematopoietic stem cells (HSCs) *ex vivo* before transplantation has been a long-standing goal in the field of hematology to improve cell therapy applications. Umbilical cord blood (CB) is an abundant and readily available stem cell source for transplantation, however, the relatively low number of hematopoietic stem- and progenitor-cells (HSPCs) in a typical CB unit currently limits the use of CB to hematopoietic cell transplantation of pediatric patients.<sup>1</sup> Successful *ex vivo* expansion of HSPCs would increase the utility of CB and allow transplantation also to adult patients. Moreover, gene-therapy applications and emerging gene-editing strategies for therapeutic targeting of HSCs would greatly benefit from robust culture conditions in which HSCs are preserved and ideally also expanded. Finally, it is likely that efforts to generate transplantable HSCs from pluripotent stem cells would be facilitated if conditions were established that allowed for the propagation of any HSCs generated.<sup>2</sup>

Submitted 26 January 2023; accepted 5 July 2023; prepublished online on *Blood Advances* First Edition 24 July 2023; final version published online 13 December 2023. <https://doi.org/10.1182/bloodadvances.2023009844>.

\*A.B. and F.E. contributed equally to this work.

Microarray data are available under the accession GSE159100. Data are available on request from the corresponding author, Jonas Larsson ([jonas.larsson@med.lu.se](mailto:jonas.larsson@med.lu.se)).

The full-text version of this article contains a data supplement.

© 2023 by The American Society of Hematology. Licensed under [Creative Commons Attribution-NonCommercial-NoDerivatives 4.0 International \(CC BY-NC-ND 4.0\)](https://creativecommons.org/licenses/by-nc-nd/4.0/), permitting only noncommercial, nonderivative use with attribution. All other rights reserved.

To date, several strategies for HSC expansion have shown promising potential, including the targeting of specific signaling pathways or epigenetic factors.<sup>3-6</sup> Moreover, the negative impact of proinflammatory signaling and oxidative stress on HSC maintenance and function has been demonstrated in other studies, as well as the importance of intracellular calcium and copper homeostasis.<sup>7-11</sup> Altogether, these efforts have led to a deeper understanding of the intricate complexity of gene regulation, signaling pathways, and metabolic networks in controlling the self-renewal and differentiation balance of HSCs.

To gain further insights into the processes governing the maintenance and propagation of human HSCs in culture, we screened several annotated small molecule libraries in primary human CB-derived HSPCs. We identified a top candidate, ciclopirox ethanolamine (CPX), which is an FDA-approved drug for the treatment of tropical fungal infections and a chelator of intracellular iron.<sup>12,13</sup> In this report, we show that CPX by reducing the intracellular labile iron pool (LIP), triggers proliferative and metabolic alterations that preserves HSC integrity and protects the stem cell pool from exhaustion during culture.

## Methods

### CB collection and CD34<sup>+</sup> cell isolation

Umbilical CB samples were collected at the end of full-term deliveries from Lund, Malmö, and Helsingborg hospitals in Sweden. Samples were collected with informed consent according to guidelines approved by the regional ethical committee. Mononuclear cells were separated from umbilical CB units through density-gradient centrifugation (LymphoprepTube, Axis-Shield Density Gradient Media #1019818) and CD34<sup>+</sup> cells were isolated using magnetic beads (#130-046-703, Miltenyi Biotec). Small molecule libraries were purchased from Enzo Life Science (specified in supplemental Table 1). Compounds tested in this study were dissolved in dimethyl sulfoxide (DMSO) and the following were added: Ciclopirox (Enzo Life Science), SR1 (STEMCELL Technologies), Ly2228820 (Selleck Chem) and UM171 (STEMCELL Technologies).

### Flow cytometry and cell sorting

Before analysis or sorting, cells were labeled with different combinations of the following fluorochrome-conjugated antihuman antibodies: CD14 (HCD14), CD19 (HIB19), CD3 (UCHT1), CD33 (P67.6), CD34 (8G12), CD38 (HIT2), CD45 (HI30), CD45RA (HI100), CD49f (GoH3), CD90 (5E10), CD133 (13A4), and CD71 (L01.1). Dead cells were excluded with 7-aminoactinomycin D (7AAD, Sigma Aldrich). Apoptotic cells were stained with the Annexin V apoptosis detection kit, according to manufacturer's protocol (BD Bioscience). All data were collected on fluorescence-activated cell sorter (FACS) Canto II or LSRII analyzer (Becton Dickinson) and analyzed with FlowJo software. Cells were sorted on a FACS Aria II or III (Becton Dickinson).

### Primary small molecule screening and dose response validation

A total of 584 small molecules at 2 concentrations (0.5 and 10 Mm; supplemental Table 1) were screened on CB CD34<sup>+</sup>

(10 000 cells), plated in U-shape 96 well plates and grown in 100  $\mu$ L of SFEM (STEMCELL Technologies) supplemented with 100 ng/mL of stem cell factor, TPO, and Flt3L (Peprotech). Cultures were kept at 37°C and 5% CO<sub>2</sub>. After 6 days, cells were washed and stained with CD34 (581) and CD90 (5E10) (BioLegend) antibodies in the same plate and analyzed by FACS Canto II. Titration experiments followed the same method. Throughout this study, culture condition and duration has been similar to the above-mentioned screen procedure.

### Human engraftment assay

All experiments with mice were reviewed and conducted under approved protocol from Lund/Malmö Local Ethical committee. Nonobese diabetic.Cg-Prkdc<sup>scid</sup>Il2rg<sup>tm1Wjl</sup>/SzJ mice (NSG; Jackson Laboratory) were sublethally irradiated (300 cGy) before transplantation. Cultured equivalent of 30 000 input CD34<sup>+</sup> cells were injected intravenously into NSG mice aged 10 to 12 weeks. Human cell contribution in Perioheral Blood (PB) and Bone Marrow (BM) of NSG was assessed at 6, 12, and 16 (for PB) and 16 weeks (for BM) after transplantation. For secondary transplantation, a half femur equivalent of BM from primary NSG recipients was injected into secondary sublethally irradiated NSG mice. Human cell contribution was assessed from 16 to 18 weeks after transplant in PB and BM. For the limit dilution analysis, BM samples were assessed at week 18 after transplant. Mice with myeloid chimerism >1% were considered engrafted for the scid repopulating cell (SRC) quantification, which was performed using Extreme Limiting Dilution Analysis online tool.<sup>14</sup>

### CFC assay

Colony-forming cell (CFC) potential was established by plating magnetically-enriched CD34<sup>+</sup> cells after 6 days of culture in presence of DMSO or CPX in methylcellulose (Methocult H4230, STEMCELL Technologies), supplemented with stem cell factor (25 ng/mL), granulocyte-macrophage colony-stimulating factor (50 ng/mL), interleukin-3 (25 ng/mL), and erythropoietin (5 U/mL, Janssen). Hematopoietic colonies were scored after 14 days.

### Cell division history assay

To assess cell division history, 1000 CD34<sup>+</sup>CD38<sup>-</sup>CD45RA<sup>-</sup>CD90<sup>+</sup> were sorted at day 0 and resuspended in 37°C warm phosphate-buffered saline (PBS). While vortexing, an equal volume of 1  $\mu$ M carboxyfluorescein succinimidyl ester (CFSE) (Sigma Aldrich #21888) solution was added to the cell suspension. After 15 minutes incubation at 37°C, the reaction was stopped by a 2-minute incubation with fetal calf serum at room temperature, and unbound CFSE was washed away twice with PBS. Cells were stained for CD34 and CD90 expression and analyzed by FACS either at day 0 or at day 6 of culture.

### Microarray analysis

Sorted, CB-derived CD34<sup>+</sup>CD38<sup>-</sup>CD90<sup>+</sup>CD45RA<sup>-</sup> cells were cultured with either CPX or DMSO. CD90<sup>+</sup> cells were resorted into RLT buffer after 24 hours and 6 days of culture. Subsequent sample processing and analysis on Affymetrix human genome U133<sup>+</sup> array were performed at KFB (Regensburg, Germany). Genes that showed a minimum of 1.5-fold modulation were considered for further analysis. Microarray data are available under the accession GSE159100.

## Intracellular iron binding measurement and iron preloading experiment

CB-CD34<sup>+</sup> cells ( $3 \times 10^4$ ) were plated and resuspended in RPMI medium containing 50 nM calcein-AM (Fisher Scientific #C3100MP) and incubated at 37°C for 5 minutes. After calcein loading, cells were washed with prewarmed PBS and plated in the presence of CPX or DMSO condition for 1 hour. Fluctuation in intracellular calcein fluorescence was measured by flow cytometry. Geometric mean fluorescence intensity was calculated by FlowJo analysis software. Iron preloading experiment was done using FAC (Sigma Aldrich) at 200 µg/mL for 1 hour. After this time, cells were spun down and new media containing CPX or DMSO were added to the culture. The experimental end point was FACS analysis of CD34 and CD90 expression at day 6.

## Sample preparation for metabolomic profiling and analysis

CB-CD34<sup>+</sup> cells ( $1 \times 10^6$ ) were treated with either CPX (1.5 µM) or control (0.1% DMSO) for 12 hours. Cells were harvested and washed with 150 mM ice-cold ammonium acetate on ice and then resuspended in 2.5 mL of fresh ice-cold ammonium acetate. Next, cells were transferred to a 15 mL polypropylene tube (BD-Falcon Cat# 352097 or Fisher Cat#14-959-70C) and spun down at 200 g for 2 minutes at 4°C. The supernatant was carefully removed, and cell pellet was resuspended in 0.75 mL of ice-cold 150 mM ammonium acetate and transferred into ice-cold cryovials. Supernatant was carefully removed, and cell pellet was snap-frozen in liquid nitrogen until metabolite profiling. Metabolite extraction and profiling was done as previously described,<sup>15</sup> and metabolites with fold changes >1.2 (CPX/DMSO) were submitted to MetaboAnalyst software v4.0.

## Extracellular flux analysis

Oxygen consumption rate (OCR) was measured on CB-CD34<sup>+</sup> cells using the XFe-96 Extracellular Flux Analyzer (Seahorse Bioscience, Agilent). Cells ( $5 \times 10^4$ ; in triplicates) were placed in 180 µL XF assay media (nonbuffered Dulbecco Modified Eagle Medium with 10 mM glucose, 2 mM Glutamax, and 1 mM sodium pyruvate) in Cell-Tak-coated plates and monitored in basal conditions and after injection of oligomycin (4 µM), FCCP (2 µM), rotenone (1 µM), and antimycin A (40 µM; Sigma). The calculations for basal respiration ( $OCR_{\text{basal}} - OCR_{\text{Rotenone/AntimycinA}}$ ), adenosine triphosphate production ( $OCR_{\text{basal}} - OCR_{\text{Oligomycin}}$ ), proton leak ( $OCR_{\text{Oligomycin}} - OCR_{\text{Rotenone/AntimycinA}}$ ), maximal respiration ( $OCR_{\text{FCCP}} - OCR_{\text{Rotenone/AntimycinA}}$ ), and spare respiratory capacity ( $OCR_{\text{FCCP}} - OCR_{\text{basal}}$ ) were performed for triplicates in each condition.

## Statistical analysis

Statistical significance was calculated using student *t* test (2-tailed) with GraphPad Prism software unless otherwise stated. For in vivo data, statistical significance was tested using Mann-Whitney nonparametric *t* test. Statistical significance in the figures are indicated by \* $P < .05$ , \*\* $P < .01$ , \*\*\* $P < .001$ , and \*\*\*\* $P < .0001$ . Error bars indicate standard error of the mean unless otherwise stated and n represents number of independent experiments.

## Results

### A small molecule screen identifies CPX as a candidate modifier of human HSCs ex vivo

To identify modifiers of human HSCs ex vivo, we first set out to define relevant phenotypic markers of CB-derived HSCs during culture as there is a dissociation between stem cell phenotype and function upon culture.<sup>16,17</sup> We monitored the expression of several stemness-related markers<sup>18</sup> in cultures of bulk CD34<sup>+</sup> cells (supplemental Figure 1A), as well as HSC-enriched CD34<sup>+</sup>CD38<sup>lo</sup>CD90<sup>+</sup>CD45RA<sup>-</sup> cells (supplemental Figure 1B) and highly purified CD34<sup>+</sup>CD38<sup>-</sup>CD90<sup>+</sup>CD45RA<sup>-</sup>CD49f<sup>+</sup> cells (supplemental Figure 1C). Cells were grown in the presence or absence of the p38α inhibitor Ly2228820 (Ly) that was previously reported to enhance HSC propagation in vitro.<sup>7</sup> Although lack of expression of both CD38 and CD45RA defines functional HSCs in freshly isolated cells, these markers are globally downregulated upon culture and not useful to further enrich HSCs from cultured cells (supplemental Figure 1A-C). Similarly, CD49f expression, which positively marks uncultured functional HSCs,<sup>18</sup> was only detected in nontransplantable CD34<sup>lo/-</sup> cells upon culture. However, both CD133<sup>19</sup> and, most notably, CD90 distinctively separated the CD34<sup>+</sup> population in all culture conditions (supplemental Figure 1A-C). Although CD133 marked a large portion (>1 out of 3) of the CD34<sup>+</sup> cells, CD90 was expressed on a discrete subset, indicating that it might define a highly enriched HSC population. Indeed, we detected robust lymph-myeloid long-term repopulating activity from the CD34<sup>+</sup>CD90<sup>+</sup> population but not from up to 10-fold higher doses of CD34<sup>+</sup>CD90<sup>-</sup> cells, regardless of starting cell population, culture time, or presence of the p38 inhibitor (supplemental Figure 1D-H). By contrast, >95% of progenitor cells with CFC potential were contained in the CD34<sup>+</sup>CD90<sup>-</sup> population (supplemental Figure 1I-J). Thus, in cultured CB cells, CD90 expression selectively marks the functional HSC pool and dissociates it from the vast majority of progenitor cells, which is in agreement with other studies.<sup>17,20-22</sup>

Having validated CD90 as a reliable marker to track human HSC activity in culture, we next performed a high-throughput screen to identify small molecules supporting the propagation of CD34<sup>+</sup>CD90<sup>+</sup> cells (supplemental Figure 2A). We screened >500 annotated compounds at 2 concentrations of 10µM and 0.5µM in CB-derived CD34<sup>+</sup> cells (supplemental Tables 1 and 2) and identified 48 primary candidates (Figure 1A-B) that increased the number of CD34<sup>+</sup>CD90<sup>+</sup> cells compared with DMSO-treated controls. Next, from titration experiments, we identified 2 compounds, the antioxidant resveratrol, as well as the antifungal and iron chelating agent CPX,<sup>23</sup> showing a particularly large increase of CD34<sup>+</sup>CD90<sup>+</sup> cells (Figure 1C). Several studies have discussed the impact of alterations in iron level and metabolism in regulation of HSPCs in normal and malignant conditions.<sup>15,24</sup> However, knowledge about the exact mechanism of iron-mediated regulation of HSPC function remains limited and therefore we selected CPX for further investigation (Figure 1D). We found that CPX was beneficial within a narrow concentration range (0.78-3.12 µM) and toxic at higher concentrations. Of note, when the screen was analyzed for an increase of total CD34<sup>+</sup> cells, CPX was not among the high-scoring compounds (supplemental Table 3). This explains why CPX had not been picked up in previous large-scale small

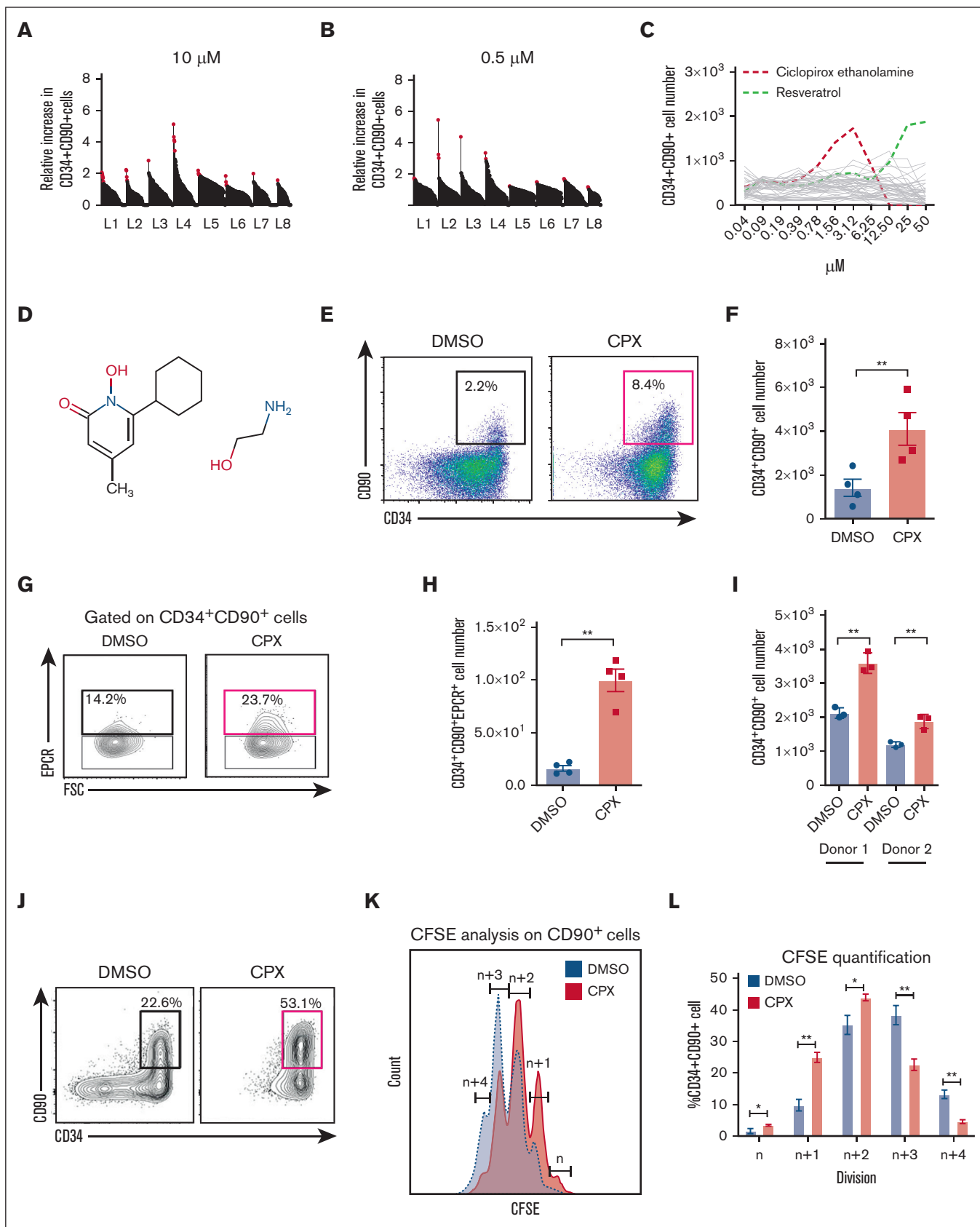


Figure 1.



molecule screens targeted at CD34<sup>+</sup> cell expansion,<sup>3,4</sup> and it further underscores the potential of our CD34<sup>+</sup>CD90<sup>+</sup> assay to detect HSC-specific outcomes independent of progenitor proliferation.

### CPX enhances the propagation of CD34<sup>+</sup>CD90<sup>+</sup> cells in cultured CB- and BM-derived HSPCs

To further validate the potential HSC-promoting activity of CPX, we first cultured bulk CB-CD34<sup>+</sup> cells for 6 days and confirmed a marked increase in both frequency and number of CD34<sup>+</sup>CD90<sup>+</sup> cells (3-fold;  $P < .01$ ) in the presence of CPX (Figure 1E-F). In addition, we also evaluated the output of CD34<sup>+</sup>CD90<sup>+</sup>EPCR<sup>+</sup> cells because EPCR expression has been associated with functional HSC activity in ex vivo cultured HSPCs.<sup>25,26</sup> Similar to CD34<sup>+</sup>CD90<sup>+</sup> cells, we could see a significant increase in the number of CD34<sup>+</sup>CD90<sup>+</sup>EPCR<sup>+</sup> cells upon CPX treatment as compared with DMSO control (Figure 1G-H). Because HSCs from different stages of ontogeny are functionally different,<sup>27</sup> we treated adult BM-derived CD34<sup>+</sup> cells with CPX and found a similar increase in CD34<sup>+</sup>CD90<sup>+</sup> cell numbers (Figure 1I). CPX did not appear to affect total cell survival as both the number of viable cells and the frequency of apoptotic cells in the CD34<sup>+</sup>CD90<sup>+</sup> population were unaltered (supplemental Figure 2B-C). Next, we tested the effect of CPX on HSC-enriched CD34<sup>+</sup>CD38<sup>-</sup>CD45RA<sup>-</sup>CD90<sup>+</sup> cells from CB and observed that it strongly preserved their immature phenotype with >50% of the cultured cells remaining CD34<sup>+</sup>CD90<sup>+</sup> after 6 days (Figure 1J). As the HSC state is typically associated with a low cellular turnover, we next asked whether CPX affected the rate of cell division of cultured CD34<sup>+</sup>CD90<sup>+</sup> cells. By tracking cell division history using CFSE labeling, we found that CPX treatment led to a slower cell division rate of CD34<sup>+</sup>CD90<sup>+</sup> cells (Figure 1K-L). By contrast, cell cycle analysis performed at day 3 did not reveal any significant changes in cell cycle distribution, indicating that the slower division rate, at least in part, may be because of prolonged cell cycle transit rather than a shift between quiescent and actively cycling states (supplemental Figure 2D).

Altogether, these data suggest that CPX selectively impedes the cell division rate of HSCs during culture and preserves their immature state.

### CPX enhances the long-term engraftment capacity of ex vivo cultured HSPCs

To evaluate the functional capability of CPX-treated cells, we cultured CD34<sup>+</sup> cells in presence of CPX or DMSO for 6 days and then assayed for colony-forming ability using methylcellulose medium. CPX-treated cells generated similar numbers of myeloid colonies (CFU-GM) and showed a trend toward higher numbers of

erythroid colonies (BFU-E) than control condition, whereas immature multilineage colonies (CFU-GEMM) were detected exclusively in the CPX-treated cultures (supplemental Figure 3A). This indicates that CPX treatment may preferentially support the more immature progenitor populations.

Next, we transplanted the cultured output of 30 000 initially seeded CB-CD34<sup>+</sup> cells into sublethally irradiated NSG mice after 6 days culture in the presence or absence of CPX in 2 separate experiments with independent batches of pooled Umbilical Cord Blood (UCB) from multiple units (Figure 2A). Mice that underwent transplantation with CPX-treated cells showed similar short-term (6 weeks) human engraftment compared with controls but displayed significantly higher engraftment 16 weeks after transplantation in peripheral blood (Figure 2B). When bone marrow was analyzed after 16 weeks, many mice displayed saturating engraftment levels (>40%), but there was still a clear trend toward higher engraftment from the CPX-treated cells in 1 experiment (Exp 1, Figure 2C) and significantly higher chimerism levels in a subsequent experiment (Exp 2, Figure 2C). The engrafted cells contributed to both myeloid and lymphoid lineages (Figure 2D-E). In order to further evaluate the impact of CPX treatment on long-term HSC repopulation ability, we transplanted BM from engrafted primary recipients into secondary NSG recipients. Eighteen weeks after transplant, we observed significantly better engraftment in the PB of the CPX group and a similar trend in BM engraftment of the secondary recipients (Figure 2F-G). Altogether, our data suggest that CPX enhances the ex vivo maintenance of functional long-term repopulating HSCs.

We further performed limit dilution analysis to be able to more accurately assess the SRC number upon treatment with CPX. Therefore, the cultured equivalents of 500, 2000, and 8000 CB-CD34<sup>+</sup> cells as well as their uncultured counterparts were transplanted into NSG mice. Human chimerism was evaluated 18 weeks after transplant and showed a trend toward an increase in number of SRCs in the CPX-treated group compared with both uncultured cells and DMSO control, adding further support to our previous transplantation experiments (supplemental Figure 3B; supplemental Table 4). Altogether, these data suggest that CPX treatment supports the propagation of functional long-term HSCs by preserving their undifferentiated state. However, it remains unresolved whether CPX treatment is sufficient to support robust expansion of bona fide HSCs in this context.

Next, we, therefore, asked whether CPX may cooperate with other molecules that recently have been reported to also enhance the short-term stem cell activity of cultured human HSPCs. Combining CPX with either the aryl hydrocarbon receptor antagonist, Stem-regenin 1 (SR1),<sup>3</sup> the p38 inhibitor Ly2228820,<sup>7</sup> or the

**Figure 1. Small molecule screening identifies CPX as a candidate modifier of human HSPCs ex vivo.** (A-B) Results from primary screening of 584 small molecules at 2 different concentrations on CB-CD34<sup>+</sup> cells. Y-axis represents the fold increase in CD34<sup>+</sup>CD90<sup>+</sup> cell number after 6 days for each compound tested, relative to DMSO control, and red dots represent selected candidates from each library (L1-L8). (C) Dose titration of 48 top candidates from the primary screen. (D) Chemical structure of CPX. (E) Representative FACS plots and (F) numbers of CD34<sup>+</sup>CD90<sup>+</sup> cells after 6 days culture of bulk CB CD34<sup>+</sup> cells (n = 4). (G) Representative FACS plot and (H) number of CD34<sup>+</sup>CD90<sup>+</sup>EPCR<sup>+</sup> cells after culture of bulk CD34<sup>+</sup> cells in presence and absence of CPX. (I) Numbers of CD34<sup>+</sup>CD90<sup>+</sup> cells after 6 days culture of human BM-CD34<sup>+</sup> cells from 2 healthy donors. (J) Representative FACS plots from 1000 CB-derived CD34<sup>+</sup>CD38<sup>-</sup>CD45RA<sup>-</sup>CD90<sup>+</sup> cells cultured for 6 days. (K) Cell division history measured by CFSE labeling on CD90<sup>+</sup> cells and (L) quantification of cell frequency in each division. Number of divisions are quantified as relative number of divisions between the 2 conditions by referring to the highest CFSE peak as n number of divisions and the subsequent peaks as n + 1, n + 2, etc.

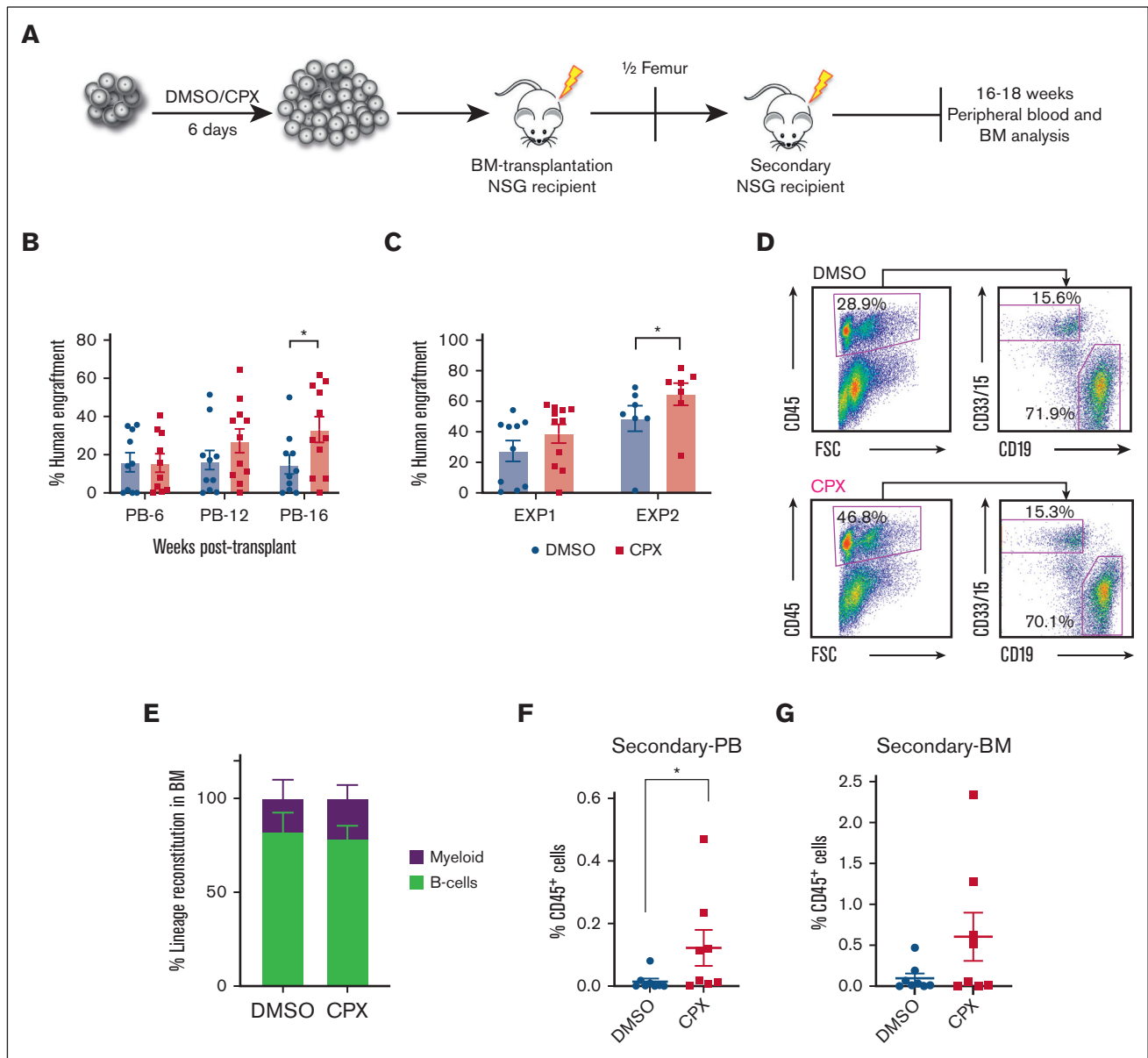


**Figure 2. CPX treatment improves long-term reconstitution capability of cultured CB-CD34<sup>+</sup> cells.** (A) Schematic representation of transplantation experiment. (B) Percentage of human CD45<sup>+</sup> cells in the PB (6, 12, 16 weeks) and (C) BM (16 weeks) of NSG recipients. (D-E) Representative FACS plots and quantification of lineage distribution for B cells (CD19) and myeloid cells (CD33/CD15) in BM. (F-G) Secondary transplantation: human chimerism level in PB (F) and BM (G) of secondary NSG recipients from 16 to 18 weeks after transplantations.

pyrimidoindole derivative UM171<sup>4</sup> led to an increase in both frequency and number of CD34<sup>+</sup>CD90<sup>+</sup> cells compared with each individual compound alone (supplemental Figure 4A), suggesting independent mechanisms of action and that the HSC-preserving activity of CPX may be beneficial together with other small molecules to promote optimal HSPC expansion. We further assessed the number of immature cells with CFU-GEMM potential that were produced from the different combinations and observed a particularly profound increase in the number of CFU-GEMM colonies when combining CPX and SR1, compared with either agent alone (supplemental Figure 4B).

### The HSC supportive effect of CPX is mediated by iron chelation

To better understand the mechanism of action of CPX on HSPCs, we performed global transcriptomic profiling on CB-CD34<sup>+</sup>CD90<sup>+</sup> cells after 24 hours or 6 days of treatment with CPX or DMSO, which identified 382 and 522 differentially expressed genes, respectively (supplemental Figure 5A). Gene set enrichment analysis on differentially expressed genes after 24 hours of CPX treatment revealed a distinct signature of reduced RNA polymerase I transcription, a rate-limiting factor for ribosomal RNA synthesis

and cell cycle progression<sup>28,29</sup> (supplemental Figure 5B; supplemental Table 5). Moreover, we observed a strong enrichment of HSC-associated gene signature in the CPX-treated CD34<sup>+</sup>CD90<sup>+</sup> cells at day 6, compared with their DMSO-treated counterparts, further indicating that the HSC state is preserved by CPX<sup>30</sup> (supplemental Figure 5C; supplemental Table 6). In addition, we could see a trend toward an enrichment of genes that are downregulated in HSCs upon *ex vivo* activation, compared with their noncultured quiescent counterparts, as reported by García-Prat et al,<sup>31</sup> suggesting that CPX-treated cells preserve some molecular features of quiescent HSCs after 6 days in culture (supplemental Figure 5D).

Further analysis of the global gene expression data from CPX-treated cells showed an enrichment of genes responsible for iron transport and uptake (supplemental Figure 5E; supplemental Table 7), which is in agreement with the well-known iron chelation activity of CPX and an indication of a compensatory response to restore the intracellular iron concentration.<sup>15,32</sup> In line with this observation, we detected an upregulation of transferrin receptor (TFRC/CD71) in CD34<sup>+</sup>CD90<sup>+</sup> cells after 6 days of treatment with CPX (Figure 3A). To assess whether CPX directly alters iron homeostasis of CB-HSPCs, we quantified free intracellular iron levels by staining CD34<sup>+</sup> cells with the cell permeable dye, Calcein-AM, whose fluorescent activity is quenched upon binding intracellular iron.<sup>33</sup> We detected a significant increase in calcein fluorescence as early as 1 hour after CPX treatment, demonstrating that CPX reduces the cytoplasmic LIP (Figure 3B). To assess whether CPX-dependent modulation of iron homeostasis was responsible for the enhanced stem cell output, we pretreated CB-CD34<sup>+</sup> cells with ferric ammonium citrate (FAC) for 1 hour before CPX treatment. We found that iron preloading, although not affecting control cells, completely reverted the CPX-induced increase of CD34<sup>+</sup>CD90<sup>+</sup> cell number (Figure 3C). In addition, iron preloading led to a substantial reduction in the number of CD90<sup>+</sup>CD71<sup>+</sup> cells after 6 days (supplemental Figure 5F). Taken together, these findings strongly suggest that the main biological effects of CPX in HSCs are mediated by its iron chelation function.

To further explore the mechanism by which iron chelation preserves the function of HSC during culture, we analyzed the metabolome of CPX-treated CB CD34<sup>+</sup> cells. We observed a reduction in biosynthesis of some amino acids and altered aminoacyl-tRNA charging, which is consistent with reduced protein synthesis and slower cell proliferation (Figure 3D; supplemental Tables 8 and 9). Furthermore, accumulation of citric acid and reduction of several intermediate metabolites such as succinic acid, malate, and fumaric acid suggested reduced activity of the tricarboxylic acid (TCA) cycle<sup>34</sup> upon CPX treatment, indicative of an altered energy-consuming state. To investigate whether CPX treatment directly affects mitochondrial respiration, we performed a mitochondrial stress test using the Seahorse extracellular flux analyzer. We observed that CPX treatment altered mitochondrial oxidative phosphorylation (OXPHOS), specifically decreasing the spare respiratory capacity compared with control but also a significant increase in the basal respiratory level (Figure 3E-F). Overall, these findings suggest that CPX-mediated iron deprivation, limits the mitochondrial respiratory mechanism and possibly restricts the transition of primitive cells toward more energy-consuming state of proliferation.

## Discussion

In this study, we developed and optimized a high content small molecule screen applied to primary human HSPCs. We show that CD90 expression directly correlates with the long-term repopulating activity of cultured CB-derived HSPCs and thus constitutes a valuable indicator of HSC content in cultured cells. From the screen, we identified CPX as a novel candidate regulator of human HSCs that promotes the *ex vivo* maintenance of cultured HSCs.

CPX is a hydroxypyridone derivative and an FDA-approved drug for the topical treatment of a wide range of fungal infections.<sup>12,35</sup> CPX has been shown to chelate intracellular iron and, thereby, affect iron-dependent proteins and cellular processes. Iron chelators have profound antileukemic activity as demonstrated in both pre-clinical and clinical investigations.<sup>23,36,37</sup> Oral administration of CPX was shown to prevent primary acute myeloid leukemia cell engraftment in nonobese diabetic/severe combined immunodeficiency mice, possibly by targeting leukemic stem cells.<sup>23</sup> However, a role of CPX in regulation of normal HSCs has not been described previously.

Here we show that CPX treatment of primary human HSPCs in culture enhanced the output of both phenotypic and functional long-term repopulating HSCs, which was associated with a slower cell division rate of the HSCs. Moreover, enrichment of HSC-associated gene signatures of *ex vivo* cultured HSCs treated with CPX point toward a direct and specific impact of CPX on the most primitive HSC population.

Upregulation of genes responsible for iron uptake and transport upon CPX treatment was quite expected given the ability of CPX on chelating intracellular LIP. This effect is considered as a compensatory response mechanism in order to restore the intracellular iron concentration. The observation that iron preloading abolished the positive impact of CPX on cultured HSPCs led us to strongly conclude that CPX-mediated stem cell stimulating effect is attributed to its iron chelating mechanism. Because iron is a vital component of many physiological systems, including iron-dependent enzymes that play a role in cell proliferation and cell cycle division, it is possible that the slower division rate of primitive CB-derived cells could be because of a mild block or lower activity of such enzymes. A similar mechanism was recently described for the thrombopoietin receptor agonist eltrombopag, known for its clinical utility in treatment of patients with bone marrow failure by stimulating multilineage hematopoiesis.<sup>15</sup> Kao et al demonstrated HSC supportive effects of eltrombopag in both mice and humans and showed that these were mediated through the iron chelation activity of eltrombopag, rather than its functions as a thrombopoietin receptor agonist.<sup>15</sup> This is consistent with our findings for CPX and consolidates the importance of intracellular iron homeostasis for HSC regulation and maintenance.

Iron is present as a cofactor in a plethora of proteins, such as iron-sulfur (Fe-S) cluster proteins and heme-containing proteins, because of its facile ability to undergo redox cycling between ferric (Fe<sup>3+</sup>) and ferrous ion (Fe<sup>2+</sup>),<sup>38</sup> and it, therefore, plays a vital role in mitochondrial respiratory complexes. In agreement with this, we found that CPX treatment affect the mitochondrial respiratory potential of HSCs mainly reducing their spare respiratory capacity. Previously, Fryknäs et al also found that iron chelation in quiescent

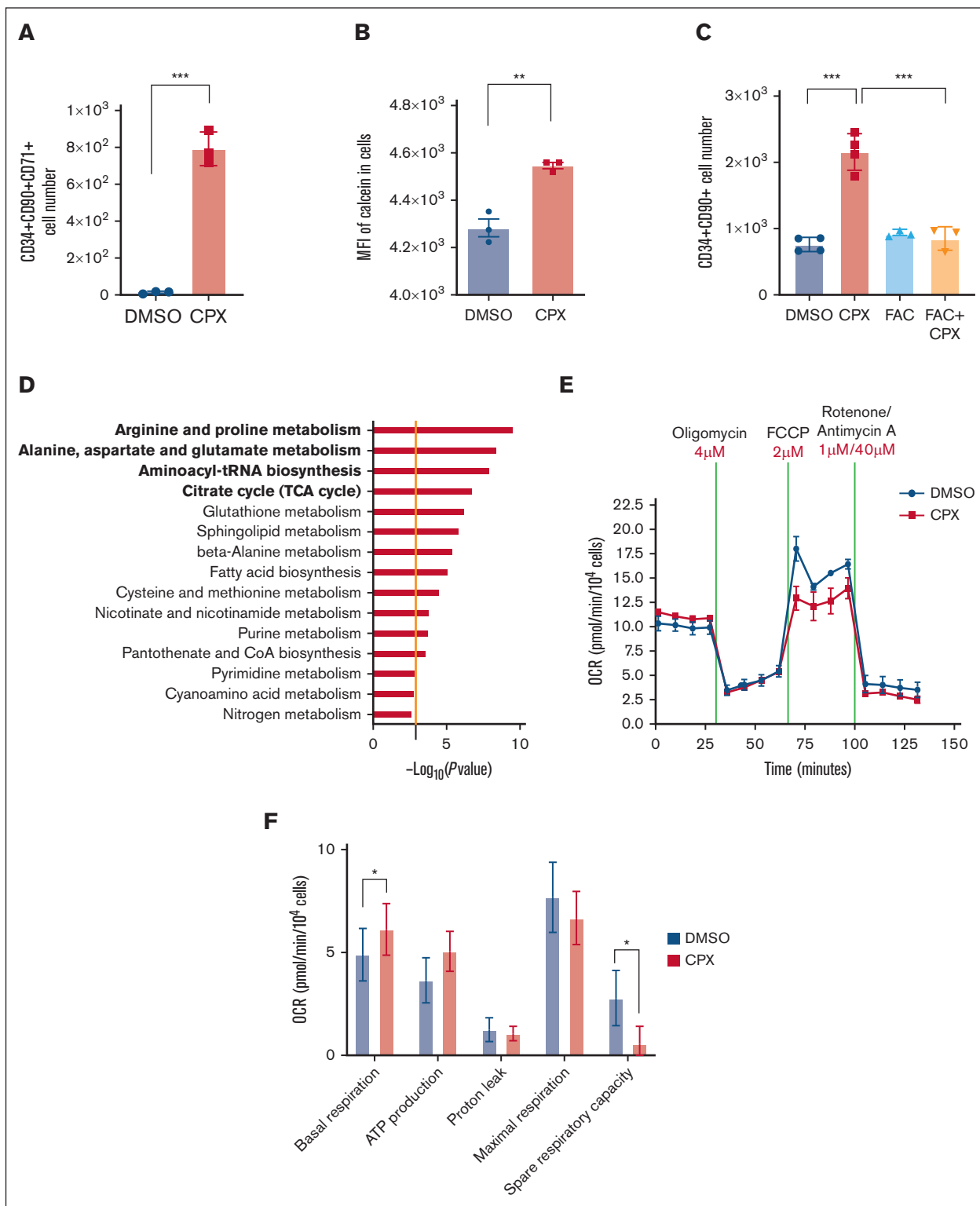


**Figure 3.** CPX induces intracellular iron deprivation that mediates the HSC supportive effect. (A) Numbers of CD34<sup>+</sup>CD90<sup>+</sup>CD71<sup>+</sup> cells after 6 days culture (n = 3). (B) Calcein-AM staining in CD34<sup>+</sup> cells treated with CPX or DMSO for 1 hour (n = 3). (C) Quantification of CD34<sup>+</sup>CD90<sup>+</sup> cell number after 6 days culture with DMSO, CPX, or ferric ammonium citrate (FAC) (n = 3). (D) Pathway analysis of altered metabolites from CB-CD34<sup>+</sup> cells treated with CPX or DMSO, the orange line represents the cutoff of significance (P = .05). (E-F) OCR measured by Seahorse assay on CB-CD34<sup>+</sup> cells.



tumor cells reduced the mitochondrial spare respiratory capacity leaving limited metabolic plasticity for cancer cells.<sup>39</sup>

Therefore, a possible scenario is that iron chelation induced by CPX delays the DNA replication as a result of the impact of iron deprivation on iron-dependent enzymes such as ribonucleotide reductase.<sup>23</sup> This is in line with altered pyrimidine and purine metabolites in our metabolome analysis, which may result in a delayed transition through the cell cycle. In addition, CPX treatment limited the mitochondrial respiratory potential of HSCs and may, thereby, introduce a road-block for the transition of quiescent HSCs toward the proliferation state that relies mainly on high oxidative energy consumption.<sup>40</sup> Therefore, CPX treatment preserves the HSC state and protects the stem cell pool from exhaustion during culture. This finding was strongly supported by CPX-mediated metabolomic changes, as evidenced by reduced level of several amino acids, alerted protein synthesis, and reduced TCA cycle activity; increased level of polyamines including spermidine and spermine is in line with a previously reported connection between polyamine levels and stemness.<sup>41</sup> In addition, we observe a reduction in S1P and other sphingolipid metabolites, which were previously reported to regulate HSCs function. Sphingolipid composition was recently reported to differ along the human hematopoietic hierarchy, and sphingolipid modulation through inhibition of sphingolipid synthesis led to an increase in functional LT-HSCs.<sup>22</sup> Collectively, we report here a previously unknown ability of CPX on preserving the immature state of human HSCs during ex vivo culture. The crucial role of iron homeostasis for human HSCs was reported recently; however, to our knowledge, here we show for the first time the impact of LIP deprivation on CB-HSC maintenance during ex vivo culture. To achieve the optimal expansion of CB-HSPCs for successful transplantation, it is of great importance to identify conditions that can robustly amplify short-term progenitor cells while maintaining and/or expanding long-term HSCs to promote hematopoietic recovery. Although our finding indicates that CPX preferentially supports the maintenance of long-term regenerative activity of cultured HSCs, it may not be sufficient in the context of robust expansion of CB-HSPCs for transplantation purposes. However, CPX in

combination with previously identified HSC expansion molecules such as SR1, P38 inhibitors, and UM171 resulted in an additional increase in the number of phenotypic HSPCs, and it will be of interest to further investigate and rigorously test combinations of CPX with these molecules for expansion of CB-HSPCs.

## Acknowledgments

This work was funded by grants from the Swedish Research Council, the Swedish Cancer Foundation, the Swedish Pediatric Cancer Foundation, Knut och Alice Wallenbergs Stiftelse, and the European Research Council under the European Union's Horizon 2020 Research and Innovation Program (grant agreement number 648894) to J.L. The work was further supported by the HematoLinné and StemTherapy programs at Lund University.

## Authorship

Contribution: M.S.T and J.L. planned the study and designed the experiments; M.S.T performed the majority of experiments with assistance from A.B, A.S., N.M., C.K., L.O., A.R., K.Z., A.G.A., J.R., and K.P.; M.S.T analyzed the data; F.E. and R.O. planned and assisted with chemical screening; Y-R.K. and B.W. performed metabolomic profiling and analyzed the data; and M.S.T and J.L. wrote the manuscript with input from the other authors.

Conflict-of-interest disclosures: The authors declare no competing financial interests.

ORCID profiles: M.S.T., 0000-0001-8429-7566; A.B., 0000-0002-3246-1819; A.S., 0000-0003-3966-3875; L.O., 0000-0003-0130-6602; A.R., 0000-0002-3404-7195; K.Z., 0000-0002-4098-0184; A.G.A., 0000-0002-0319-4416; K.P., 0000-0001-6738-4705; R.O., 0000-0002-7107-3472; B.W., 0000-0002-9534-6690.

Correspondence: Jonas Larsson, Molecular Medicine and Gene Therapy, Lund Stem Cell Center, Lund University, BMC A12, 221 84, Lund, Sweden; email: [jonas.larsson@med.lu.se](mailto:jonas.larsson@med.lu.se).

## References

1. Broxmeyer HE. Enhancing the efficacy of engraftment of cord blood for hematopoietic cell transplantation. *Transfus Apher Sci*. 2016;54(3):364-372.
2. Lee J, Dykstra B, Sackstein R, Rossi DJ. Progress and obstacles towards generating hematopoietic stem cells from pluripotent stem cells. *Curr Opin Hematol*. 2015;22(4):317-323.
3. Boitano AE, Wang J, Romeo R, et al. Aryl hydrocarbon receptor antagonists promote the expansion of human hematopoietic stem cells. *Science*. 2010;329(5997):1345-1348.
4. Fares I, Chagraoui J, Gareau Y, et al. Cord blood expansion. Pyrimidoindole derivatives are agonists of human hematopoietic stem cell self-renewal. *Science*. 2014;345(6203):1509-1512.
5. Delaney C, Heimfeld S, Brashem-Stein C, Voorhies H, Manger RL, Bernstein ID. Notch-mediated expansion of human cord blood progenitor cells capable of rapid myeloid reconstitution. *Nat Med*. 2010;16(2):232-236.
6. Chaurasia P, Gajzer DC, Schaniel C, D'Souza S, Hoffman R. Epigenetic reprogramming induces the expansion of cord blood stem cells. *J Clin Invest*. 2014;124(6):2378-2395.
7. Baudet A, Karlsson C, Safaee Talkhoncheh M, Galeev R, Magnusson M, Larsson J. RNAi screen identifies MAPK14 as a druggable suppressor of human hematopoietic stem cell expansion. *Blood*. 2012;119(26):6255-6258.
8. Safaee Talkhoncheh M, Agatheeswaran Saubramaniam, Mattias Magnusson, Praveen Kumar, Jonas Larsson, Aurélie Baudet. Transient inhibition of NF-kappaB signaling enhances ex vivo propagation of human hematopoietic stem cells. *Haematologica*. 2018;103(9):1444-1450.

9. Mantel CR, O'Leary HA, Chitteti BR, et al. Enhancing hematopoietic stem cell transplantation efficacy by mitigating oxygen shock. *Cell*. 2015;161(7):1553-1565.
10. Luchsinger LL, Strikoudis A, Danzl NM, et al. Harnessing hematopoietic stem cell low intracellular calcium improves their maintenance in vitro. *Cell Stem Cell*. 2019;25(2):225-240.e7.
11. Peled T, Landau E, Mandel J, et al. Linear polyamine copper chelator tetraethylenepentamine augments long-term ex vivo expansion of cord blood-derived CD34+ cells and increases their engraftment potential in NOD/SCID mice. *Exp Hematol*. 2004;32(6):547-555.
12. Sehgal VN. Ciclopirox: a new topical pyrodonium antimycotic agent. A double-blind study in superficial dermatomycoses. *Br J Dermatol*. 1976;95(1):83-88.
13. Zhou H, Shen T, Luo Y, et al. The antitumor activity of the fungicide ciclopirox. *Int J Cancer*. 2010;127(10):2467-2477.
14. Hu Y, Smyth GK. ELDA: extreme limiting dilution analysis for comparing depleted and enriched populations in stem cell and other assays. *J Immunol Methods*. 2009;347(1-2):70-78.
15. Kao YR, Chen J, Narayanagari SR, et al. Thrombopoietin receptor-independent stimulation of hematopoietic stem cells by eltrombopag. *Sci Transl Med*. 2018;10(458):eaas9563.
16. Dorrell C, Gan OI, Pereira DS, Hawley RG, Dick JE. Expansion of human cord blood CD34(+)CD38(-) cells in ex vivo culture during retroviral transduction without a corresponding increase in SCID repopulating cell (SRC) frequency: dissociation of SRC phenotype and function. *Blood*. 2000;95(1):102-110.
17. Danet GH, Lee HW, Luongo JL, Simon MC, Bonnet DA. Dissociation between stem cell phenotype and NOD/SCID repopulating activity in human peripheral blood CD34(+) cells after ex vivo expansion. *Exp Hematol*. 2001;29(12):1465-1473.
18. Notta F, Doulatov S, Laurenti E, Poeppl A, Jurisica I, Dick JE. Isolation of single human hematopoietic stem cells capable of long-term multilineage engraftment. *Science*. 2011;333(6039):218-221.
19. Yao CL, Feng YH, Lin XZ, Chu IM, Hsieh TB, Hwang SM. Characterization of serum-free ex vivo-expanded hematopoietic stem cells derived from human umbilical cord blood CD133(+) cells. *Stem Cells Dev*. 2006;15(1):70-78.
20. Tomellini E, Fares I, Lehnertz B, et al. Integrin-alpha3 Is a functional marker of ex vivo expanded human long-term hematopoietic stem cells. *Cell Rep*. 2019;28(4):1063-1073.e5.
21. Ansari U, Tomellini E, Chagraoui J, et al. CEACAM1 is a novel culture-compatible surface marker of expanded long-term reconstituting hematopoietic stem cells. *Blood Adv*. 2022;6(12):3626-3631.
22. Xie SZ, Garcia-Prat L, Voisin V, et al. Sphingolipid modulation activates proteostasis programs to govern human hematopoietic stem cell self-renewal. *Cell Stem Cell*. 2019;25(5):639-653.e7.
23. Eberhard Y, McDermott SP, Wang X, et al. Chelation of intracellular iron with the antifungal agent ciclopirox olamine induces cell death in leukemia and myeloma cells. *Blood*. 2009;114(14):3064-3073.
24. Isidori A, Loscocco F, Visani G, et al. Iron toxicity and chelation therapy in hematopoietic stem cell transplant. *Transplant Cell Ther*. 2021;27(5):371-379.
25. Fares I, Chagraoui J, Lehnertz B, et al. EPCR expression marks UM171-expanded CD34(+) cord blood stem cells. *Blood*. 2017;129(25):3344-3351.
26. Subramaniam A, Talkhoncheh MS, Magnusson M, Larsson JJ. Endothelial protein C receptor (EPCR) expression marks human fetal liver hematopoietic stem cells. *Haematologica*. 2019;104(2):e47-e50.
27. Mayani H. Biological differences between neonatal and adult human hematopoietic stem/progenitor cells. *Stem Cells Dev*. 2010;19(3):285-298.
28. Russell J, Zomerdijk JC. RNA-polymerase-I-directed rDNA transcription, life and works. *Trends Biochem Sci*. 2005;30(2):87-96.
29. Comai L. Mechanism of RNA polymerase I transcription. *Adv Protein Chem*. 2004;67:123-155.
30. Laurenti E, Doulatov S, Zandi S, et al. The transcriptional architecture of early human hematopoiesis identifies multilevel control of lymphoid commitment. *Nat Immunol*. 2013;14(7):756-763.
31. Garcia-Prat L, Kaufmann KB, Schneiter F, et al. TFEB-mediated endolysosomal activity controls human hematopoietic stem cell fate. *Cell Stem Cell*. 2021;28(10):1838-1850.e10.
32. Seiser C, Posch M, Thompson N, Kuhn LC. Effect of transcription inhibitors on the iron-dependent degradation of transferrin receptor mRNA. *J Biol Chem*. 1995;270(49):29400-29406.
33. Breuer W, Epsztejn S, Millgram P, Cabantchik IZ. Transport of iron and other transition metals into cells as revealed by a fluorescent probe. *Am J Physiol*. 1995;268(6 Pt 1):C1354-1361.
34. Martinez-Reyes I, Chandel NS. Mitochondrial TCA cycle metabolites control physiology and disease. *Nat Commun*. 2020;11(1):102.
35. Shen T, Huang S. Repositioning the old fungicide ciclopirox for new medical uses. *Curr Pharm Des*. 2016;22(28):4443-4450.
36. Kaloyannidis P, Yannaki E, Sakellari I, et al. The impact of desferrioxamine postallogeic hematopoietic cell transplantation in relapse incidence and disease-free survival: a retrospective analysis. *Transplantation*. 2010;89(4):472-479.
37. Fukushima T, Kawabata H, Nakamura T, et al. Iron chelation therapy with deferasirox induced complete remission in a patient with chemotherapy-resistant acute monocytic leukemia. *Anticancer Res*. 2011;31(5):1741-1744.
38. Lill R. Function and biogenesis of iron-sulphur proteins. *Nature*. 2009;460(7257):831-838.

39. Fryknäs M, Zhang X, Bremberg U, et al. Iron chelators target both proliferating and quiescent cancer cells. *Sci Rep.* 2016;6:38343.
40. Simsek T, Kocabas F, Zheng J, et al. The distinct metabolic profile of hematopoietic stem cells reflects their location in a hypoxic niche. *Cell Stem Cell.* 2010;7(3):380-390.
41. Minguzzi M, Guidotti S, Platano D, et al. Polyamine supplementation reduces DNA damage in adipose stem cells cultured in 3-D. *Sci Rep.* 2019;9(1):14269.